Neuro-Oncology

Neuro-Oncology 18(5), 735–743, 2016
doi:10.1093/neuonc/nov268
Advance Access date 3 November 2015

Large-volume low apparent diffusion coefficient lesions predict poor survival in bevacizumab-treated glioblastoma patients

Myron Zhang†, Bryanna Gulotta†, Alissa Thomas, Thomas Kaley, Sasan Karimi, Igor Gavrilovic, Kaitlin M. Woo, Zhigang Zhang, Julio Arevalo-Perez, Andrei I. Holodny, Marc Rosenblum, and Robert J. Young

Department of Radiology, Memorial Sloan Kettering Cancer Center, New York, New York (M.Z., B.G., S.K., J.A.-P., A.I.H., R.J.Y.); Department of Neurology, Memorial Sloan Kettering Cancer Center, New York, New York (A.T., T.K., I.G.); Department of Epidemiology and Biostatistics, Memorial Sloan Kettering Cancer Center, New York, New York (K.M.W., Z.Z.); Department of Pathology, Memorial Sloan Kettering Cancer Center, New York, New York (M.R.); Brain Tumor Center, Memorial Sloan Kettering Cancer Center, New York, New York (T.K., S.K., I.G., A.I.H., M.R., R.J.Y.)

Corresponding Author: Robert J Young, MD, Neuroradiology Service, Department of Radiology, Memorial Sloan Kettering Cancer Center, 1275 York Avenue, New York, New York 10065 USA (youngr@mskcc.org).

†These authors contributed equally as co-first authors.

Background. Glioblastomas treated with bevacizumab may develop low-signal apparent diffusion coefficient (low-ADC) lesions, which may reflect increased tumor cellularity or atypical necrosis. The purpose of this study was to examine the relationship between low-ADC lesions and overall survival (OS). We hypothesized that growing low-ADC lesions would be associated with shorter OS.

Methods. We retrospectively identified 52 patients treated with bevacizumab for the first ($n = 42$, 81%) or later recurrence of primary glioblastoma, who had low-ADC lesions and 2 post-bevacizumab scans ≤90 days apart. Low-ADC lesion volumes were measured, and normalized 5th percentile histogram low-ADC values were recorded. Using OS as the primary endpoint, semiparametric Cox models were fitted to ascertain univariate and multivariate hazard ratios (HRs) with significance at $P = .05$.

Results. Median OS was 9.1 months (95% CI = 7.2–14.3). At the second post-bevacizumab scan, the volume of the low-ADC lesion (median: 12.94 cm^3) was inversely associated with OS, with larger volumes predicting shorter OS (HR = 1.014 [95% CI = 1.003–1.025], $P = .009$). The percent change in low-ADC volume (median: 6.8%) trended toward increased risk of death with growing volumes ($P = .08$). Normalized 5th percentile low-ADC value and its percent change were not associated with OS ($P > .51$). Also correlated with shorter OS were the pre-bevacizumab nonenhancing volume ($P = .025$), the first post-bevacizumab enhancing volume ($P = .040$), and the second post-bevacizumab enhancing volume ($P = .004$).

Conclusions. The volume of low-ADC lesions at the second post-bevacizumab scan predicted shorter OS. This suggests that low-ADC lesions may be considered important imaging markers and included in treatment decision algorithms.

Keywords: apparent diffusion coefficient, (ADC), bevacizumab, diffusion, glioblastoma.

Glioblastomas are the most common malignant primary brain tumors in the United States.[1] These tumors secrete high levels of vascular endothelial growth factor (VEGF) that promote angiogenesis and vascular permeability to drive tumor progression.[2–4] Bevacizumab is a humanized recombinant monoclonal antibody that blocks the binding of VEGF to its tyrosine kinase receptors, Flt1 and KDR, on endothelial cells.[5–7] Bevacizumab has been shown to decrease neovascularity and permeability of the blood-brain barrier and induce normalization of remaining tumoral vessels.[5,8,9] In patients with recurrent glioblastoma, studies have also demonstrated improvements in radiographic response, progression-free survival (PFS) and symptoms after treatment with bevacizumab.[8–14]

Bevacizumab may induce rapid and potent suppression of enhancement due to VEGF-mediated effects upon the vasculature even without actual antitumor activity. This phenomenon may explain the observed modest, inconsistent improvements in overall survival (OS) despite prolongations in PFS, which are

Received 14 April 2015; accepted 1 October 2015
© The Author(s) 2015. Published by Oxford University Press on behalf of the Society for Neuro-Oncology. All rights reserved. For permissions, please e-mail: journals.permissions@oup.com.

determined based on clinical and imaging criteria.[15] Determining progression of disease (PD) in bevacizumab-treated glioblastomas is often difficult due to the suppression of enhancement that may result in pseudoresponse rather than true tumor response.[16,17] This limitation was recognized by the widely adopted Response Assessment in Neuro-Oncology (RANO) response criteria, which added a significant increase in nonenhancing disease as a new criterion for PD.[18] In the setting of antiangiogenic therapy, not only is the relationship between enhancement and active tumor imperfect, evaluation of change in the size of an enhancing mass is also unreliable. Therefore, there has been great interest in applying functional imaging techniques to characterize tumor activity more accurately.

Diffusion-weighted imaging (DWI) is an advanced MRI technique that allows in vivo quantification of water motion. The parameter of water diffusion is independent from the parameters involved in enhancement (ie, microvascular density, neoangiogenesis, blood-brain barrier disruption),[19,20] suggesting that it may have a role in patients receiving antiangiogenic therapy. Increased diffusion restriction manifests as low signal intensity on apparent diffusion coefficient (ADC) maps (low-ADC) and has been correlated with high tumor cellularity and upregulated VEGF.[21,22] In contrast, elevated diffusion manifests as high signal intensity on ADC maps (high-ADC) and has been correlated with treatment-induced and tumor growth-induced necrosis and disruptions in cellular integrity.[23–25] Researchers have suggested that bevacizumab may prolong PFS in patients with necrotic tumors and high ADC lesions more than in patients with nonnecrotic tumors.[26] Interestingly, Mong et al.[27] also described a subset of bevacizumab-treated patients with glioblastoma with stable low-ADC lesions as having improved outcomes, viewing the low-ADC lesions as a reflection of unique, bevacizumab-related gelatinous necrosis rather than highly cellular tumor. In our clinical practice, we have observed growing low-ADC lesions in bevacizumab-treated glioblastomas. The purpose of this study was to examine the changes in these low-ADC lesions over time and their possible implications for OS. We hypothesized that growing low-ADC lesions would predict poor OS.

Materials and Methods

Study Design

This retrospective study was granted a waiver of informed consent by the local Institutional Review Board. The study was conducted in a manner compliant with Health Insurance Portability and Accountability Act (HIPAA) regulations and with the approval of the hospital Privacy Board.

Patient Population

Inclusion criteria for our study were as follows: (i) treatment received for primary glioblastoma consisting of surgical resection and standard partial brain radiation therapy (RT) with concomitant and adjuvant temozolomide chemotherapy; (ii) treatment with bevacizumab for recurrent tumor; (iii) first and second post-bevacizumab MRI scans performed $\leq$90 days apart; and (iv) presence of one or more low-ADC lesions on the post-bevacizumab MRI scans, as determined by visual inspection. Bevacizumab was administered at standard doses of 10 mg/kg intravenously every 2 weeks. Patients who received bevacizumab as part of their initial treatment regimen (ie, before tumor recurrence) were excluded from the study, as were patients who received alternative chemotherapy regimens. From an institutional database, we retrospectively identified a total of 164 consecutive patients with primary glioblastoma treated with bevacizumab over an 18-month period from January 2009 to June 2010. As summarized in Figure 1, 52 cases were eligible for inclusion in this study. Full chart reviews were performed by an experienced neuro-oncologist to determine the patients' treatment course including date of diagnosis, surgical resection, RT, chemotherapy, dates of disease progression, date of death, and clinical variables including age and Karnofsky performance scale (KPS).

Diffusion-weighted Imaging: Acquisition and Analysis

MRI scans were obtained using 1.5-Tesla and 3-Tesla magnets (Signa Excite/HDx and Discovery 450/750, GE Healthcare). Axial DWI was acquired using a single-shot echo-planar imaging sequence with an acquisition with $b = 0$ and 3 diffusion-weighted acquisitions with $b = 1000$ s/mm^2.

Two trained operators (each with 1 year of experience in MRI postprocessing) performed ADC analyses under the direct supervision of a board-certified neuroradiologist who holds a Certificate of Added Qualification in Neuroradiology (with 15 years of experience). The DWI and axial contrast-enhanced T1-weighted images were transferred to an off-line workstation and analyzed using available commercial software (nordicICE, NordicNeuroLab). ADC maps were calculated from the DWI, co-registered with the contrast-enhanced T1-weighted images, and then displayed as overlays. For each scan, a region-of-interest (ROI) was manually delineated around the low-signal lesion on every axial ADC slice. The ROIs were visually verified to include only high-signal areas on the DWI and were also compared against the remaining standard MRI images to exclude hemorrhage and nonenhancing cystic or necrotic areas, although the ADC maps were only explicitly co-registered to the contrast-enhanced T1-weighted images. The low-ADC lesions were always located within the tumor-related fluid-attenuated inversion recovery (FLAIR) hyperintense abnormality. The set of ROIs was then integrated to construct a volume-of-interest (VOI) of the low-ADC lesion recorded in cubic centimeters. The ADC values from the VOI were binned into a histogram and then normalized using the mean ADC obtained from an ROI placed in the contralateral normal-appearing white matter. From the normalized ADC histogram, the bottom 5th percentile was calculated and recorded as the normalized 5th percentile low-ADC value.[28,29] The percent change was calculated between the pre-bevacizumab and first post-bevacizumab scans as [(first post scan)-(pre scan)]/(pre scan), and between the second post-bevacizumab and first post-bevacizumab scans as [(second post scan)-(first post scan)]/(first post scan).

In patients who underwent resection of their low-ADC lesions, the preoperative or last MRI was analyzed, and a VOI was constructed around the low-ADC lesion. The values were binned into a histogram, and the mean low-ADC value was

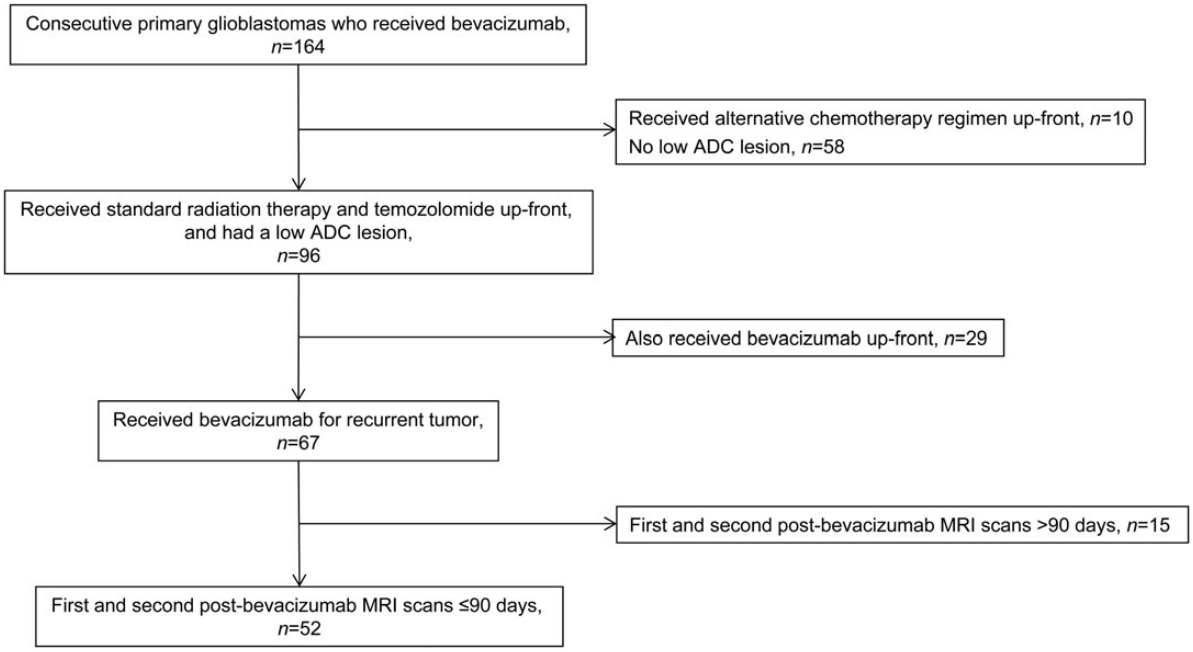

Fig. 1. Summary of study cohort.

recorded. For these patients, the mean low-ADC values were not normalized as per LaViolette et al.[30]

Enhancing and Nonenhancing Acquisition and Analysis

Standard multiplanar T1-weighted, T2-weighted, FLAIR, and contrast-enhanced T1-weighted images were also obtained, along with gradient echo ($n = 20$) or susceptibility-weighted ($n = 19$) images. In every patient, a neuroradiologist blinded to the DWI and ADC maps examined the MRI scans, and a VOI was manually constructed around the enhancing tumor while excluding vessels, hemorrhage, and mineralization. A VOI was also manually constructed around the nonenhancing lesion based on the FLAIR images. The VOIs of the enhancing tumor and nonenhancing lesion were recorded in cubic centimeters. The nonenhancing lesion may consist of solid nonenhancing tumor, infiltrating tumor cells, and/or bland edema; although the powerful anti-VEGF and antiedema effects of bevacizumab probably render nonenhancing tumor the predominant constituent at the first and second post-bevacizumab scans.

Statistical Analysis

The primary endpoint was survival, with OS calculated from the bevacizumab start date to the date of death. Age, low-ADC volume and percent change, ADC values and percent change, enhancing volume and percent change, and nonenhancing volume and percent change were all expressed as continuous variables. KPS score ($\geq$80 vs $<$80) and whether patients were treated at first or subsequent progressions were incorporated as dichotomous variables. In order to incorporate multiple clinical factors, semiparametric Cox models were fitted to ascertain univariate and multivariate HRs. Kaplan-Meier curves were constructed to show the OS versus the percent change in low-ADC volume, as dichotomized by the median change. Candidate clinical factors and imaging factors at the second post-bevacizumab scan with $P < .10$ on univariate analysis were incorporated into a multivariate analysis model in a stepwise selection process. To reduce potential systematic underestimation of the rate ratio,[31,32] we also calculated an immortal time bias corrected OS (OS_{ITBC}) from the date of the second post-bevacizumab scan. To evaluate changes in low-ADC volume, Fisher' exact tests were used. For all analyses and 95% confidence intervals, statistical significance was 2-sided with $P = .05$. Statistical analyses were performed using R (version 3.0.1; R Development Core Team) with the "survival" package.

Results

Patient Characteristics

As summarized in Table 1, the 52 patients in the study cohort had a median age of 62.7 years with 31 (60%) men and 21 (40%) women. Of the 46 patients with known KPS, the majority of patients ($n = 34$, 74%) had KPS $\geq$ 80. Most patients received bevacizumab for first progression ($n = 42$, 81%). The median time from starting bevacizumab to the first post-bevacizumab scan was 42 days (range: 7–108 d) and from the first to the second post-bevacizumab scan was 14 days (range: 7–70 d).

Low-ADC Lesion Analysis

A low-ADC lesion was present before bevacizumab in the nearly two-thirds of the patients ($n = 34$, 65.4%). As summarized in Table 2, the median low-ADC lesion volume at the pre-bevacizumab scan was 12.82 cm^3 (range: 0.70–167.39), at the first post-bevacizumab scan was 15.20 cm^3 (range: 0.41–146.07)

Table 1. Patient demographics and treatments

	N (%)
Patients with confirmed glioblastoma	52
Median age, range (y)	62, 28–80
Median KPS, range	90, 50–100
KPS < 80	12 (23)
KPS ≥ 80	34 (65)
KPS missing	6 (12)
Men	31 (60)
Women	21 (40)
Progression	
First progression	42 (81)
Second or later progression	10 (19)
Median weeks on bevacizumab (range)	24 (7–105)
Adjuvant therapy	
Concurrent with bevacizumab[a]	36 (69)
After stopping bevacizumab[b]	12 (23)
Reason for stopping bevacizumab	
Progression of disease or death	47 (90)
Adverse event related to bevacizumab[c]	5 (10)

[a]Treatments concurrent with bevacizumab: temozolomide ($n = 15$), carboplatin ($n = 12$), carmustine ($n = 12$), lomustine ($n = 4$), lapatinib ($n = 3$), etoposide ($n = 3$), irinotecan ($n = 1$), and radiation therapy ($n = 2$). Several patients received multiple sequential regimens concurrent with bevacizumab ($n = 16$).
[b]Treatments following bevacizumab: carboplatin ($n = 3$), carmustine ($n = 2$), etoposide ($n = 2$), temozolomide ($n = 2$), gamma-knife radiosurgery ($n = 1$); and clinical trials: (sorafenib and tipifarnib [$n = 2$], cediranib and cilengitide [$n = 1$], cabozantinib [$n = 1$], perifosine and temsirolimus [$n = 1$], and dendritic cell vaccination [$n = 1$]). Several patients received multiple regimens after discontinuation of bevacizumab ($n = 4$).
[c]Adverse events included: hypertension ($n = 2$), intracranial hemorrhage ($n = 1$), pulmonary embolism ($n = 1$), and myocardial infarction ($n = 1$).

and at the second post-bevacizumab scan was 12.94 cm^3 (range: 0.67–263.90). Low-ADC lesions larger than the median volume at the second post-bevacizumab scan were also larger at the first post-bevacizumab scan ($P < .001$). The median volume change to the first post-bevacizumab scan from the pre-bevacizumab scan was −7.0% (range: −79.7% to 406.9%), and to the second post-bevacizumab scan from the first post-bevacizumab scan was 6.8% (range: −95.2% to 1, 117.0%), with no correlation for the volume changes between scans ($P \geq .26$). The median normalized 5th percentile low-ADC values and the changes at the first and second post-bevacizumab scans were not significant ($P \geq .52$). A representative case is shown in Figure 2.

Pathology of the low-ADC lesion was available for 4 patients after gross total resection ($n = 2$), subtotal resection ($n = 1$), or autopsy ($n = 1$). All 4 patients showed persistent/recurrent tumor: 3 patients had only tumor as illustrated in Figure 3, and one patient had tumor admixed with necrotizing treatment effects. In these 4 patients, the mean low-ADC value was 0.828×10^{-3} mm^2/s (range: 0.775–0.878).

Low-ADC Survival Analysis

As summarized in Table 2, survival analysis showed that all patients died during follow-up with median OS of 9.1 months (95% CI = 7.2–14.3). In univariate analyses, the absolute volume of the low-ADC lesion at the second post-bevacizumab scan was a significant predictor of OS, with larger volumes associated with shorter OS (HR = 1.014 [95% CI = 1.003–1.025], $P = .009$). The other metrics were not statistically significant ($P > .11$) including the normalized 5th percentile low-ADC value ($P = .52$) and the change in normalized 5th percentile low-ADC ($P = .71$). When the change in low-ADC volume was dichotomized by the median 6.8%, there was no difference in survival (HR = 1.16 [95%CI = 0.69–2.11], $P = .51$). There was no difference in OS between patients who had low-ADC lesions before bevacizumab ($n = 26$, 50%) or who developed low-ADC lesions after beginning bevacizumab ($P = .60$).

The top 3 clinical and second post-bevacizumab scan factors from the univariate analysis (age, low-ADC volume, and Δ low-ADC volume) were selected for the final multivariate analysis, which showed that only low-ADC volume remained a significant predictor of OS (HR = 1.01 [95% CI = 1.002–1.024], $P = .019$).

When calculating OS_{ITBC} from the second post-bevacizumab scan in order to minimize immortal time bias, the median OS_{ITBC} was 6.1 months (95% CI = 4.4–11.5). The absolute volume of the low-ADC lesion remained a predictor of OS_{ITBC} at univariate (HR = 1.015 [95% CI = 1.010–1.030], $P = .003$) and multivariate (HR = 1.014 [95% CI = 1.003–1.020], $P = .009$) analysis. The percent change in low-ADC volume from the first to the second post-bevacizumab scan showed a small trend toward a higher risk of death for patients with growing volumes (HR = 1.001 [95% CI = 0.999–1.003], $P = .08$), while the other metrics were not significant ($P \geq .51$).

Enhancing and Nonenhancing Survival Analysis

At the pre-bevacizumab scan, the volume of the nonenhancing lesion was a significant predictor of OS (HR = 1.004 [95% CI = 1.000–1.008], $P = .025$), while the other parameters including the volume of the enhancing lesion were not ($P \geq .22$).

At the first post-bevacizumab scan, the volume of the enhancing tumor was a significant predictor of OS (HR = 1.015 [95% CI = 1.001–1.029], $P = .040$), while the other parameters including percent change were not ($P \geq .11$). At the second post-bevacizumab scan, in addition to the volume of the low-ADC lesion described above ($P = .009$), the volume of the enhancing tumor was again a significant predictor of OS (HR = 1.017 [95% CI = 1.005–1.028], $P = .004$), while the other parameters were not ($P \geq .11$).

Discussion

In patients with glioblastoma treated with bevacizumab for progression, we found that larger low-ADC volume lesions at the second post-bevacizumab scan correlated with worse OS. For each 1 cm^3 increase in low-ADC volume from the observed range (median = 12.94 cm^3, simplified to 13 cm^3 in this discussion), there was a 1.4% increase in the risk of death. For example, a theoretical spherical tumor at the second post-bevacizumab

Table 2. Summary of results, with hazard ratios and *P* values calculated for overall survival from start of bevacizumab therapy

	Median (range)	HR[c] (95% CI)	*P* Value
Age		0.983 (0.959–1.008)	.19
KPS (<80 vs ≥80)	–	1.159 (0.571–2.354)	.68
First vs later progression	–	1.077 (0.528–2.197)	.84
Low-ADC lesion present before beginning bevacizumab	–	1.160 (0.663–2.030)	.60
Pre-bevacizumab scan			
Nonenhancing volume, cm^3	120.71 (14.36–412.04)	1.004 (1.000–1.008)	.025[d]
Enhancing volume, cm^3	29.61 (1.76–87.59)	1.007 (0.996–1.020)	.22
Low-ADC volume, cm^3	12.82 (0.70–167.39)	0.998 (0.987–1.009)	.73
Normalized 5th percentile low-ADC	1.018 (0.510–1.633)	1.112 (0.242–5.119)	.89
First post-bevacizumab scan[a]			
Nonenhancing volume, cm^3	64.18 (5.90–269.88)	1.001 (0.996–1.007)	.60
Δ Nonenhancing volume	−48.7% (−94.1–475.0)	1.000 (0.995–1.006)	.95
Enhancing volume, cm^3	13.58 (0.07–85.88)	1.015 (1.001–1.029)	.040[d]
Δ Enhancing volume	−46.8% (−99.5–305.4)	1.004 (0.999–1.009)	.11
Low-ADC volume, cm^3	15.20 (0.41–146.07)	1.010 (0.999–1.020)	.36
Δ Low-ADC volume	−7.0% (−79.7–406.9)	1.000 (0.999–1.004)	.37
Normalized 5th percentile low-ADC	0.884 (0.452–1.246)	1.066 (0.171–6.635)	.95
Δ Normalized 5th percentile low-ADC	−13.2% (−44.4–108.5)	1.002 (0.988–1.016)	.78
2nd post-bevacizumab scan[b]			
Nonenhancing volume, cm^3	53.14 (2.72–490.49)	1.004 (0.999–1.008)	.11
Δ Nonenhancing volume	−0.6% (−95.2–188.4)	1.006 (0.998–1.013)	.12
Enhancing volume, cm^3	10.47 (0.01–120.89)	1.017 (1.005–1.028)	.004[d]
Δ Enhancing volume	−10.0% (−93.6–1,193.6)	1.000 (0.999–1.002)	.74
Low-ADC volume, cm^3	12.94 (0.66–263.87)	1.014 (1.003–1.025)	.009[d]
Δ Low-ADC volume	6.8% (−95.2–1,116.8)	1.001 (0.999–1.002)	.26
Normalized 5th percentile low-ADC	0.904 (0.020–1.925)	0.57 (0.11–3.06)	.52
Δ Normalized 5th percentile low-ADC	1.6% (−98.2–178.3)	1.000 (0.999–1.010)	.71

Abbreviations: ADC, apparent diffusion coefficient; CI, confidence interval; HR, hazard ratio.
[a]Δ calculated from pre-bevacizumab.
[b]Δ calculated from first post-bevacizumab.
[c]HR per 1 cm^3 increase from the median 13 cm^3.
[d]Statistically significant.

scan with diameter = 4 cm (radius = 2 cm) that has a volume of 33.5 cm^3 (volume = $^4/_3\pi$[radius]^3) would have a 33% increase in risk of death (HR = $[1.014]^{20.5}$). It is notable, however, that a 25% increase in the product of bidimensional diameters qualifying as progressive disease according to the RANO criteria[18] is equivalent to a 40% increase in volume and would rapidly increase the risk of death based on the absolute volume. These results suggest that low-ADC lesions may be a marker for tumor and shorter survival, analogous to the manner in which enhancing lesions have been associated with increased risk of death.[33]

Low-ADC values have been correlated with increased tumor cellularity, glioma grade, cellular proliferation, and ischemia.[21,34–36] In untreated tumors, cellularity is likely the primary contributor to low-ADC values and may predict tumor progression and worse prognosis.[26,36–39] With treatment, multiple other factors contribute to low-ADC values including cell death, necrosis, edema, gliosis, hemorrhage, and/or mineralization, all of which may affect the Brownian movement of water. In bevacizumab-treated tumors, imaging and pathologic studies suggest a competing mechanism of tumor hypoxia due to insufficient vascular proliferation.[36,40] Hypoxia is a powerful stimulant of tumor growth and invasiveness.[41,42] Growth of the nonenhancing tumor with bevacizumab therapy may be due to stimulation of invasive tumor cells by bevacizumab and/or to failure of bevacizumab to target tumor cells that are not dependent on angiogenesis.[11,43,44]

Researchers have reported that pretreatment ADC assessments are helpful in identifying patients likely to respond to bevacizumab.[26,37] Our results indicate that ADC assessments during treatment are also helpful, with larger low-ADC volumes at the second post-bevacizumab scan predicting shorter survival. A recent paper by Mong et al[27] described stable low-ADC volumes as a favorable prognostic marker. In their study of patients with high-grade gliomas receiving bevacizumab who had low-ADC lesions present for at least 2 months, they found prolonged time to progression (median 248 d vs. 159 d) and prolonged OS (mean 1676 d vs. 633 d) as compared with matched controls without low-ADC lesions. Aside from 2 patients who showed doubling of median volume over 6 months, most patients (90%) demonstrated stable volumes over 6 months. Three-fourths of their low-ADC lesions developed

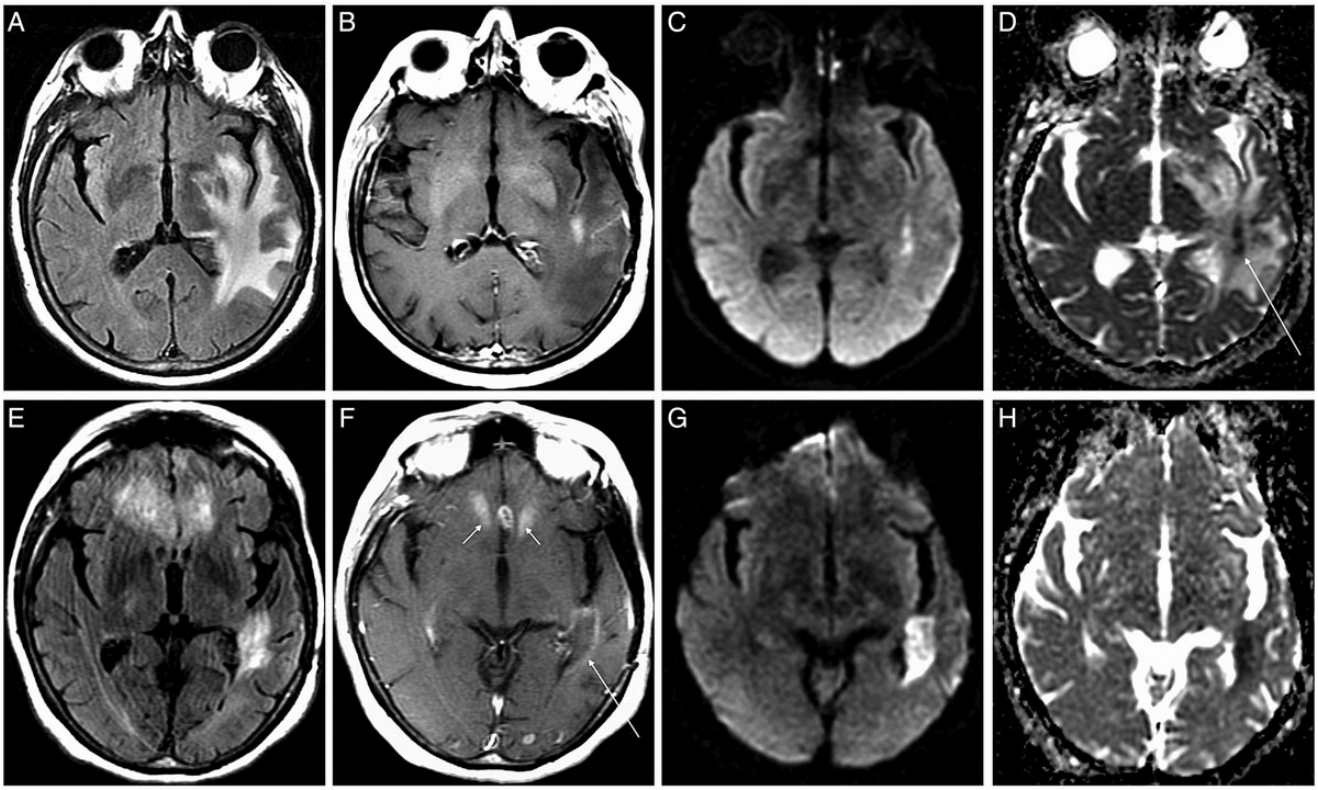

Fig. 2. Representative low-apparent diffusion coefficient (ADC) lesion. Axial fluid-attenuated inversion recovery (FLAIR) (A) contrast T1-weighted, (B) diffusion-weighted imaging, (C) and ADC ,(D) images at first post-bevacizumab scan and corresponding images at second post-bevacizumab scan (E-H). Representative glioblastoma showing a small enhancing lesion in the left peritrigonal region with low-ADC signal (arrow, D). Two months later, the peritrigonal lesion shows increased low-ADC volume (H) There is also mild ill-defined peripheral enhancement, which is typical with antiangiogenic therapy (low arrow, F), and multifocal enhancing lesions in the anterior corpus callosum and frontal lobes (double arrows, F) that did not show low-ADC signal. The peritrigonal lesion had a 93% increase in low-ADC volume, and the patient expired 2.1 months after the second scan.

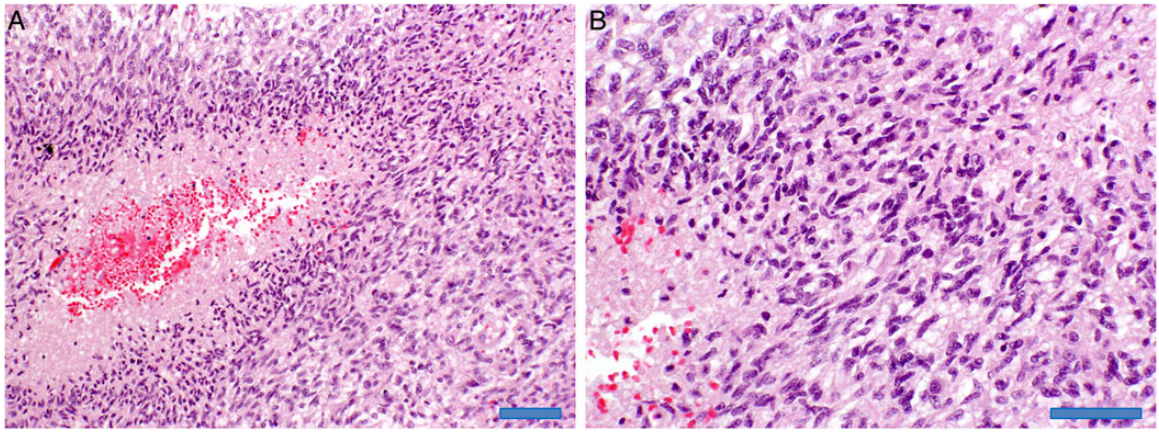

Fig. 3. Autopsy section. Hematoxylin-eosin staining at 20× magnification (A, scale bar is 100 μm) reveals recurrent classic glioblastoma histology with dense tumor cellularity and necrosis with perinecrotic pseudopalisading (left). The 40× magnification (B, scale bar is 50 μm) confirms dense tumor cellularity and necrosis (lower left).

after initiation of bevacizumab. In addition, their sample of patients with glioma was more heterogeneous than ours, with only two-thirds having glioblastoma ($n = 14$) and only four-fifths being treated for recurrence. Their results suggest that low-ADC lesions preselected for stability tended to remain stable (ie, patients preselected as bevacizumab

responders with stable low-ADC tumors demonstrated improved survival).

Other authors have also examined low-ADC lesions in glioma patients treated with bevacizumab and described atypical gelatinous, coagulative, or calcified necrosis at pathology.[27,30,45–47] In 2 high-grade glioma patients treated with bevacizumab, LaViolette et al[30] described low-ADC values (0.593 and 0.637×10^{-3} mm^2/s) in areas of diffusion-restricted necrosis at autopsy that were significantly lower than low-ADC values (0.643 and 0.786×10^{-3} mm^2/s) in adjacent areas of hypercellular tumor. Repeat pathology confirmed tumor in the low-ADC lesions for 4 of our patients— with mean low-ADC values comparable to those reported by LaViolette et al—but they do not help confirm the presence of extra-low-ADC values in bevacizumab-related necrosis. In the non-bevacizumab literature, the opposite has been reported, with low-ADC values described as lower in hypercellular recurrent gliomas than in treatment-related necrosis.[48,49] While we acknowledge that some low-ADC lesions may represent bevacizumab-related necrosis, we postulate that some large and growing low-ADC volumes, as observed in our cohort, might instead represent cellular and/or hypoxic glioblastoma. In the few patients ($n =$ 4, 7.7%) in our cohort who had post-bevacizumab pathology available for analysis, we found clear evidence of recurrent tumor in every case. Admittedly, given the small sample size, it is possible that some or many of our low-ADC lesions may also have represented co-existing or only bevacizumab-related necrosis (as one of the pathology cases showed both recurrent tumor and treatment necrosis). Furthermore, we acknowledge that we have observed individual patients with large low-ADC lesions occasionally survive for long periods of time without further progression, as described by other authors.[27] It is possible that these entities represent a spectrum, with progressively lower ADC-values occurring with non-bevacizumab related necrosis, then non-bevacizumab-related or bevacizumab-related tumor, and finally bevacizumab-related necrosis. The coexistence of these entities may explain why we did not detect a survival difference based on change in volume of the low-ADC lesion between scans, as both necrosis and tumor may expand during bevacizumab treatment. Nevertheless, our results show that in a group-wise analysis, large low-ADC volumes are correlated with shorter survival. Additional research with pathologic correlation in larger numbers of patients is necessary to better understand the origin(s) and implications of these low-ADC lesions with and without bevacizumab therapy.

We did not detect a correlation between change in the normalized 5th percentile low-ADC values and OS. This result contrasts with the findings of Jain et al,[50] who detected decreasing low-ADC values in 20 progressive recurrent gliomas (80% of which were glioblastomas) treated with bevacizumab but not in nonprogressing gliomas. To measure absolute ADC values, they drew VOIs on contrast T1-weighted and FLAIR images to encompass enhancing and nonenhancing tumor. Those VOIs were then co-registered to the ADC maps to obtain absolute measurements. In contrast, our VOIs were identified and drawn directly on the ADC maps and verified against the DWI and contrast T1-weighted images. Our 5th percentile low-ADCs were also normalized to the contralateral brain. These subtle methodological differences may explain why we detected no correlation. By focusing primarily on the low-ADC lesions, however, we were able to demonstrate a correlation between absolute volume and OS. This suggests that diffusion imaging has an important role in the evaluation of glioblastomas on bevacizumab and that ADC results should be considered when making treatment management decisions, despite their omission from standardized response criteria. While the etiology of low-ADC lesions often remains unclear, we propose that large low-ADC lesions be viewed as suspicious for cellular and/or hypoxic tumor and as possible predictors of shorter survival, especially when they are growing in size. Lesions that are stable, even if they are large, could be followed closely, given the possibility of atypical gelatinous necrosis and longer survival. Further functional characterization of these low-ADC lesions by perfusion or spectroscopic MRI or PET scanning may be helpful in determining their etiology and need for treatment.

While the purpose of this study was to examine the implications of the low-ADC lesions in patients receiving bevacizumab therapy, we also found the nonenhancing volume at the pre-bevacizumab scan ($P = .025$) and the enhancing volumes at the first and second post-bevacizumab scans ($P = .040$ and .004, respectively) to predict shorter OS. The changes in nonenhancing volumes and enhancing volumes between scans, however, were not significant ($P \geq .11$). Kickingereder et al[51] also reported that enhancing and nonenhancing volumes and their respective changes at first follow-up were predictors of 6-month PFS and 12-month OS ($P \leq .02$) in bevacizumab-treated recurrent glioblastomas. Two-dimensional estimates of enhancing and nonenhancing disease are already incorporated into the RANO criteria.[18] Our low-ADC results are particularly important because DWI provides unique functional data about tumor biology; therefore, the status of these low-ADC lesions at the second post-bevacizumab scan may be useful as an independent imaging biomarker for predicting patient survival. While the low-ADC results were only applicable at the second post-bevacizumab scan, after the nonenhancing and enhancing results at the pre-bevacizumab and first post-bevacizumab scans, they offer the advantage of directly providing prognostic information from the visually apparent diffusion abnormalities.

Several potential limitations were encountered. First, because this was a retrospective observational study, histopathologic evaluation of the low-ADC lesions was possible in only a minority of patients. In addition, by requiring patients to have had 2 MRI scans <3 months after beginning bevacizumab, we may have excluded patients who progressed rapidly or otherwise did not survive to a second scan. Second, the ADC lesions varied in some patients from homogeneously low in signal to heterogeneously low and high in signal. In the latter case, we relied on the volumetric histogram analysis to minimize potential operator bias in lesion selection and filter for the smallest low-ADC values. Third, we did not specifically compare the low-ADC analysis with other proposed imaging biomarkers such as dynamic contrast susceptibility contrast (DSC) perfusion.[51,52] While these perfusion methods are increasing in popularity, their acquisition and analysis are varied, while DWI is part of the standard brain protocol at most imaging centers and therefore remains the most widely performed functional sequence. Since we did not detect a correlation between the low-ADC values and OS, our results suggest that visual analysis of low-ADC lesions and estimates of lesion

volumes are sufficient to quickly estimate HRs. Lastly, we used OS as the primary endpoint. While not susceptible to the subjective definitions that may limit common surrogates such as PFS, OS may be affected by the timing of first versus second or later recurrence, and the efficacy of subsequent salvage therapies. Further complicating estimates of survival, some of our neuro-oncologists may have changed treatment based on the growing low-ADC volumes. We observed similar results whether we calculated OS from the start of bevacizumab treatment or OS_{ITBC} from the second post-bevacizumab scan intended to reduce potential lead-time survivor bias.

In conclusion, we found that low-ADC lesion volumes in bevacizumab-treated glioblastomas were inversely associated with survival, and there was a trend toward shorter survival for patients with growing low-ADC lesions. Histogram quantification of low-ADC values, however, did not correlate with patient outcome. These results suggest that visually apparent large low-ADC lesions in patients being treated with bevacizumab may be considered important prognostic imaging markers and included in treatment decision algorithms, to prompt close follow-up or potential consideration for new treatment options or modifications.

Funding

MZ was supported by the Memorial Sloan Kettering Cancer Center Medical Student Summer Fellowship Program. KMW and ZZ were partly supported by National Institutes of Health MSK Cancer Center Support Grant/Core Grant P30 CA008748. JAP was supported by a grant from the Spanish foundation, Fundación Alfonso Martín Escudero.

Acknowledgments

The authors are grateful for the expert editorial advice of Ms. Ada Muellner.

Conflict of interest statement. None declared.

References

1. Ostrom QT, Gittleman H, Farah P, et al. CBTRUS statistical report: Primary brain and central nervous system tumors diagnosed in the United States in 2006–2010. *Neuro Oncol*. 2013;15(suppl 2): 1–56.
2. Dvorak HF. Vascular permeability factor/vascular endothelial growth factor: A critical cytokine in tumor angiogenesis and a potential target for diagnosis and therapy. *J Clin Oncol*. 2002; 20(21):4368–4380.
3. O'Connor JPB, Carano RAD, Clamp AR, et al. Quantifying antivascular effects of monoclonal antibodies to vascular endothelial growth factor: insights from imaging. *Clin Cancer Res*. 2009;15(21):6674–6682.
4. Zagzag D, Lukyanov Y, Lan L, et al. Hypoxia-inducible factor 1 and VEGF upregulate CXCR4 in glioblastoma: implications for angiogenesis and glioma cell invasion. *Lab Invest*. 2006;86(12): 1221–1232.
5. Batchelor TT, Duda DG, di Tomaso E, et al. Phase II study of cediranib, an oral pan-vascular endothelial growth factor receptor tyrosine kinase inhibitor, in patients with recurrent glioblastoma. *J Clin Oncol*. 2010;28(17):2817–2823.
6. Plate KH, Breier G, Weich HA, Risau W. Vascular endothelial growth factor is a potential tumour angiogenesis factor in human gliomas in vivo. *Nature*. 1992;359(6398):845–848.
7. Stefanik DF, Fellows WK, Rizkalla LR, et al. Monoclonal antibodies to vascular endothelial growth factor (VEGF) and the VEGF receptor, FLT-1, inhibit the growth of C6 glioma in a mouse xenograft. *J Neurooncol*. 2001;55(2):91–100.
8. Friedman HS, Prados MD, Wen PY, et al. Bevacizumab alone and in combination with irinotecan in recurrent glioblastoma. *J Clin Oncol*. 2009;27(28):4733–4740.
9. Lai A, Tran A, Nghiemphu PL, et al. Phase II study of bevacizumab plus temozolomide during and after radiation therapy for patients with newly diagnosed glioblastoma multiforme. *J Clin Oncol*. 2011;29(2):142–148.
10. Kreisl TN, Kim L, Moore K, et al. Phase ii trial of single-agent bevacizumab followed by bevacizumab plus irinotecan at tumor progression in recurrent glioblastoma. *J Clin Oncol*. 2009;27(5): 740–745.
11. Chamberlain MC. Bevacizumab for the treatment of recurrent glioblastoma. *Clin Med Insights Oncol*. 2011;5:117–129.
12. Vredenburgh JJ, Desjardins A, Herndon JE, et al. phase ii trial of bevacizumab and irinotecan in recurrent malignant glioma. *Clin Cancer Res*. 2007;13(4):1253–1259.
13. Kreisl TN, Kim L, Moore K, et al. Phase II trial of single-agent bevacizumab followed by bevacizumab plus irinotecan at tumor progression in recurrent glioblastoma. *J Clin Oncol*. 2009;27(5): 740–745.
14. Vredenburgh JJ, Desjardins A, Herndon JE 2nd, et al. Bevacizumab plus irinotecan in recurrent glioblastoma multiforme. *J Clin Oncol*. 2007;25(30):4722–4729.
15. Chinot OL, Wick W, Mason W, et al. Bevacizumab plus radiotherapy-temozolomide for newly diagnosed glioblastoma. *N Engl J Med*. 2014;370(8):709–722.
16. Iwamoto FM, Abrey LE, Beal K, et al. Patterns of relapse and prognosis after bevacizumab failure in recurrent glioblastoma. *Neurology*. 2009;73(15):1200–1206.
17. Brandsma D, van den Bent MJ. Pseudoprogression and pseudoresponse in the treatment of gliomas. *Curr Opin Neurol*. 2009;22(6):633–638.
18. Wen PY, Macdonald DR, Reardon DA, et al. Updated response assessment criteria for high-grade gliomas: response assessment in neuro-oncology working group. *J Clin Oncol*. 2010;28(11): 1963–1972.
19. Svolos P, Kousi E, Kapsalaki E, et al. The role of diffusion and perfusion weighted imaging in the differential diagnosis of cerebral tumors: a review and future perspectives. *Cancer Imaging*. 2014;14:20.
20. Mabray MC, Barajas RF Jr., Cha S. Modern brain tumor imaging. *Brain Tumor Res Treat*. 2015;3(1):8–23.
21. Sugahara T, Korogi Y, Kochi M, et al. Usefulness of diffusion-weighted MRI with echo-planar technique in the evaluation of cellularity in gliomas. *J Magn Reson Imaging*. 1999;9(1): 53–60.
22. Brat DJ, Van Meir EG. Vaso-occlusive and prothrombotic mechanisms associated with tumor hypoxia, necrosis, and accelerated growth in glioblastoma. *Lab Invest*. 2004;84(4): 397–405.

23. Chenevert TL, Sundgren PC, Ross BD. Diffusion imaging: insight to cell status and cytoarchitecture. *Neuroimaging Clin N Am*. 2006; 16(4):619–632, viii-ix.
24. Mardor Y, Roth Y, Ochershvilli A, et al. Pretreatment prediction of brain tumors' response to radiation therapy using high b-value diffusion-weighted MRI. *Neoplasia*. 2004;6(2):136–142.
25. Prager AJ, Martinez N, Beal K, Omuro A, Zhang Z, Young RJ. Diffusion and perfusion MRI to differentiate treatment-related changes including pseudoprogression from recurrent tumors in high-grade gliomas with histopathologic evidence. *AJNR Am J Neuroradiol*. 2015;36(5):877–885.
26. Pope WB, Kim HJ, Huo J, et al. Recurrent glioblastoma multiforme: ADC histogram analysis predicts response to bevacizumab treatment. *Radiology*. 2009;252(1):182–189.
27. Mong S, Ellingson BM, Nghiemphu PL, et al. Persistent diffusion-restricted lesions in bevacizumab-treated malignant gliomas are associated with improved survival compared with matched controls. *AJNR Am J Neuroradiol*. 2012;33(9):1763–1770.
28. Ryu YJ, Choi SH, Park SJ, Yun TJ, Kim JH, Sohn CH. Glioma: application of whole-tumor texture analysis of diffusion-weighted imaging for the evaluation of tumor heterogeneity. *PLoS One*. 2014;9(9):e108335.
29. Tozer DJ, Jager HR, Danchaivijitr N, et al. Apparent diffusion coefficient histograms may predict low-grade glioma subtype. *NMR Biomed*. 2007;20(1):49–57.
30. LaViolette PS, Mickevicius NJ, Cochran EJ, et al. Precise ex vivo histological validation of heightened cellularity and diffusion-restricted necrosis in regions of dark apparent diffusion coefficient in 7 cases of high-grade glioma. *Neuro Oncol*. 2014; 16(12):1599–1606.
31. Suissa S. Immortal time bias in pharmaco-epidemiology. *Am J Epidemiol*. 2008;167(4):492–499.
32. Suissa S. Immortal time bias in observational studies of drug effects. *Pharmacoepidemiol Drug Saf*. 2007;16(3):241–249.
33. Iliadis G, Kotoula V, Chatzisotiriou A, et al. Volumetric and MGMT parameters in glioblastoma patients: survival analysis. *BMC Cancer*. 2012;12:3. doi: 10.1186/1471-2407-12-3.
34. Higano S, Yun X, Kumabe T, et al. Malignant astrocytic tumors: clinical importance of apparent diffusion coefficient in prediction of grade and prognosis. *Radiology*. 2006;241(3):839–846.
35. Castillo M, Smith JK, Kwock L, Wilber K. Apparent diffusion coefficients in the evaluation of high-grade cerebral gliomas. *AJNR Am J Neuroradiol*. 2001;22(1):60–64.
36. Gupta A, Young RJ, Karimi S, et al. Isolated diffusion restriction precedes the development of enhancing tumor in a subset of patients with glioblastoma. *AJNR Am J Neuroradiol*. 2011;32(7): 1301–1306.
37. Pope WB, Lai A, Mehta R, et al. Apparent diffusion coefficient histogram analysis stratifies progression-free survival in newly diagnosed bevacizumab-treated glioblastoma. *Am J Neuroradiol*. 2011;32(5):882–889.
38. Barajas RF Jr., Rubenstein JL, Chang JS, Hwang J, Cha S. Diffusion-weighted MR imaging derived apparent diffusion coefficient is predictive of clinical outcome in primary central nervous system lymphoma. *AJNR Am J Neuroradiol*. 2010;31(1): 60–66.
39. Kobus T, Vos PC, Hambrock T, et al. Prostate cancer aggressiveness: in vivo assessment of MR spectroscopy and diffusion-weighted imaging at 3T. Radiology. 2012;265(2):457–467.
40. Kleinschmidt-Demasters BK, Damek DM. The imaging and neuropathological effects of Bevacizumab (Avastin) in patients with leptomeningeal carcinomatosis. *J Neurooncol*. 2010;96(3): 375–384.
41. Keunen O, Johansson M, Oudin A, et al. Anti-VEGF treatment reduces blood supply and increases tumor cell invasion in glioblastoma. *Proc Natl Acad Sci USA*. 2011;108(9):3749–3754.
42. Gerstner ER, Frosch MP, Batchelor TT. Diffusion magnetic resonance imaging detects pathologically confirmed, nonenhancing tumor progression in a patient with recurrent glioblastoma receiving bevacizumab. *J Clin Oncol*. 2010;28(6): e91–e93.
43. Chamberlain MC. Bevacizumab plus irinotecan in recurrent glioblastoma. *J Clin Oncol*. 2008;26(6):1012–1013; Author reply 1013.
44. Pope WB, Xia Q, Paton VE, et al. Patterns of progression in patients with recurrent glioblastoma treated with bevacizumab. *Neurology*. 2011;76(5):432–437.
45. Hesselink JR, Barkovich MJ, Seibert TM, et al. Bevacizumab: radiation combination produces restricted diffusion on brain MRI. *CNS Oncol*. 2014;3(5):329–335.
46. Farid N, Almeida-Freitas DB, White NS, et al. Restriction-Spectrum Imaging of Bevacizumab-Related Necrosis in a Patient with GBM. *Front Oncol*. 2013;3:258. doi: 10.3389/fonc.2013.00258.
47. Bahr O, Harter PN, Weise LM, et al. Sustained focal antitumor activity of bevacizumab in recurrent glioblastoma. *Neurology*. 2014;83(3):227–234.
48. Hein PA, Eskey CJ, Dunn JF, Hug EB. Diffusion-weighted imaging in the follow-up of treated high-grade gliomas: tumor recurrence versus radiation injury. *AJNR Am J Neuroradiol*. 2004;25(2): 201–209.
49. Zeng QS, Li CF, Liu H, Zhen JH, Feng DC. Distinction between recurrent glioma and radiation injury using magnetic resonance spectroscopy in combination with diffusion-weighted imaging. *Int J Radiat Oncol Biol Phys*. 2007;68(1):151–158.
50. Jain R, Scarpace LM, Ellika S, et al. Imaging response criteria for recurrent gliomas treated with bevacizumab: role of diffusion weighted imaging as an imaging biomarker. *J Neurooncol*. 2010; 96(3):423–431.
51. Kickingereder P, Wiestler B, Burth S, et al. Relative cerebral blood volume is a potential predictive imaging biomarker of bevacizumab efficacy in recurrent glioblastoma. *Neuro Oncol*. 2015;17(8):1139–1147.
52. Schmainda KM, Zhang Z, Prah M, et al. Dynamic susceptibility contrast MRI measures of relative cerebral blood volume as a prognostic marker for overall survival in recurrent glioblastoma: results from the ACRIN 6677/RTOG 0625 multicenter trial. *Neuro Oncol*. 2015;17(8):1148–1156.